Available online at www.sciencedirect.com
SCIENCE DIRECT
Journal of Power Sources 150 (2005) 255–260
JOURNAL OF POWER SOURCES
www.elsevier.com/locate/jpowsour

$Y(OH)_3$-coated $Ni(OH)_2$ tube as the positive-electrode materials of alkaline rechargeable batteries

Fang-Yi Cheng, Jun Chen *, Pan-Wen Shen

Institute of New Energy Materials Chemistry, Nankai University, Tianjin 300071, PR China

Received 11 January 2005; received in revised form 21 February 2005; accepted 28 February 2005
Available online 13 June 2005

Abstract

$Y(OH)_3$-coated $Ni(OH)_2$ tubes with mesoscale dimensions were synthesized by a two-step chemical precipitation method under ambient conditions. The products were characterized using X-ray diffraction (XRD), scanning electron microscopy (SEM), transmission electron microscopy (TEM) and high-resolution TEM (HRTEM) equipped with energy dispersive spectroscopy (EDS). The instrumental analyses showed that the size of the tubes was of mesoscale dimension and the proportion of the tube morphology was about 95%. The as-prepared $Y(OH)_3$-coated $Ni(OH)_2$ tubes were further used as the active material of alkaline rechargeable batteries. The electrochemical studies revealed that the composite tubes exhibited superior electrode performance such as high discharge capacity, good redox reversibility and excellent charge–discharge properties at high-temperature and high-discharge rate. The reason for the working mechanism is also discussed, showing that the tube hollow structure plays important roles in optimizing the performance of the $Y(OH)_3$-coated $Ni(OH)_2$ tube electrodes.

Keywords: Nickel hydroxide; Yttrium hydroxide; Composite tube; Alkaline rechargeable batteries

1. Introduction

Rechargeable batteries play more and more important roles in daily life, especially in power tools, portable electronics and electric vehicles [1,2]. Nickel hydroxide is widely used as the active material for the positive electrode of Ni-based alkaline rechargeable batteries (e.g. Fe/Ni, Zn/Ni, Cd/Ni and MH/Ni) due to its high power density, good cycling ability, and relatively low price [3]. For reasons of proper recombination reactions and safety, the capacities of the Ni-based alkaline rechargeable batteries are usually positive-electrode limited, and this suggests that improving the properties of the nickel hydroxide electrode is essential to promote the performance of such batteries.

The overall electrochemical reactions occurring at a usual reversible nickel electrode can simply be written as the equation that follows:

$$Ni(OH)_2 + OH^- \rightleftharpoons NiOOH + H_2O + e^- \quad (1)$$

Traditionally, the theoretical capacity of the nickel hydroxide is believed to be $289\,mAh\,g^{-1}$ if the electrode reaction involves one-electron transfer. However, the charge–discharge reactions, which actually take place in the nickel hydroxide electrode, are much more complex. It has been reported that four structural types of nickel hydroxides and oxyhydroxides exist during the lifetime of a nickel hydroxide electrode, namely, β-$Ni(OH)_2$, β-NiOOH, γ-Ni(OH), and α-$Ni(OH)_2$ [4]. The nickel oxidation state in γ-NiOOH is known to exceed 3 because of Ni^{4+} defect [5], thus $Ni(OH)_2$ can yield a higher discharge capacity than $289\,mAh\,g^{-1}$. However, the formation of these phases leads to volume expansion or swelling of the electrode, and then particle contact due to these phases change increases the resistance of the electrode reaction, especially at high-rate or high-temperature charge/discharge [6]. To improve the characteristics of the nickel hydroxide electrode, much research

* Corresponding author. Tel.: +86 22 2350 6808; fax: +86 22 2350 9118.
E-mail address: chenabc@nankai.edu.cn (J. Chen).

0378-7753/$ – see front matter © 2005 Elsevier B.V. All rights reserved.
doi:10.1016/j.jpowsour.2005.02.073

has been focused on the development of spherical $Ni(OH)_2$ powder, employing additives such as cobalt, aluminum, and rare-earth-based oxides and hydroxides [7–11]. The addition of yttrium shows great influence on the performance of the batteries under high-temperature [12]. It has also been reported that nickel hydroxide with a smaller crystalline size exhibits superior electrochemical behaviors [13,14]. However, the core of spherical nickel hydroxide powder is still inactive because of the diffusion barrier. In comparison, $Ni(OH)_2$ tubes in mesoscale dimensions facilitate proton diffusion and exhibit excellent electrochemical performance such as high capacity and cycling stability [15]. However, in high power application such as electric vehicles, the development of nickel-based electrodes is limited by the critical requirement of high-temperature and high discharge–charge rate performance. Therefore, although numerous studies have been carried out in order to improve the characteristics of nickel hydroxide electrodes, the results are still not complete. In particular, the utilization of the active materials at high-temperatures, which is very critical for battery application in electric vehicles, limits further development for nickel electrodes.

In this work, the $Y(OH)_3$-coated $Ni(OH)_2$ tubes were prepared by a two-step chemical precipitation method using porous alumina membranes as the template. The electrochemical properties of the as-prepared product was further tested and the results showed that the $Y(OH)_3$-coated $Ni(OH)_2$ composite tubes in mesoscale dimensions were promising active materials for the positive electrodes of alkaline rechargeable batteries.

2. Experimental

2.1. Synthesis and characterization of $Y(OH)_3$-coated $Ni(OH)_2$ tubes

The $Ni(OH)_2$ tubes coated with 5 wt.% $Y(OH)_3$ were prepared using a two-step chemical deposition process. Anodic aluminum oxide membranes (Whatman, Ø47 mm with 0.2 μm pores and 60 μm thickness) were used as the templates. $Ni(NO_3)_2{\cdot}6H_2O$, $Y(NO_3)_3{\cdot}6H_2O$, ammonia, and other reagents were all of analytical grade and used without further purification. In a typical synthesis, an alumina template was gently immersed in 0.1 M $Y(NO_3)_3{\cdot}6H_2O$ aqueous solution for 3 h and then was taken out to remove the solution on the template surface. Ammonia (0.5 M) was slowly dripped onto the membrane, and the ammonia solution gradually penetrated the template to react with $Y(NO_3)_3$. This solution filling and $Y(OH)_3$ precipitation procedure was repeated several times to form the tubes in the template pores. Then the similar procedure was carried out for $Ni(OH)_2$ deposition except for longer reaction time and higher solution concentration. After that, the membrane was dissolved by 2 M NaOH solution to remove the alumina. The product was collected by filtration, washed with deionized water, and dried at 60 °C in vacuum for 2 h. The reactions involved in the preparation process can be expressed as

Nanotube preparation:

$$Y(NO_3)_3 \cdot 6H_2O + 3NH_4OH \rightarrow Y(OH)_3 + 3NH_4NO_3 + 6H_2O$$

$$Ni(NO_3)_2 \cdot 6H_2O + 2NH_4OH \rightarrow Ni(OH)_2 + 2NH_4NO_3 + 6H_2O$$

Template dissolution:

$$Al_2O_3 + 2NaOH \rightarrow 2NaAlO_2 + H_2O$$

The as-synthesized samples were characterized by powder X-ray powder diffraction (Rigaku INT-2000 X-ray generator, Cu Kα radiation), scanning electron microscopy (Philips XL-30, 20 kV), transmission electron microscopy (TEM) and high-resolution TEM (Philips Tecnai F20, 200 KV) equipped with energy dispersive spectroscopy.

2.2. Electrochemical measurement

Nickel hydroxide electrodes were prepared by inserting an active paste into a nickel foam substrate. A paste containing 85 wt.% active materials (5 wt.% $Y(OH)_3$-coated nickel hydroxide powders), 10 wt.% carbon black, and 5 wt.% polytetrafluoroethylene (PTFE) was used. The electrode was dried at 80 °C for 1 h and cut into disk (1.2 cm × 1.2 cm), which was pressed at a pressure of 100 kg cm^{-2} to a thickness of 0.4 mm. The electrode was spot-welded to a nickel sheet for electrical connection. Electrochemical measurements were performed using a Solartron SI 1260 Potentionstat Analyzer with 1287 Interface and an Arbin charge/discharge unit at controlled temperatures in an electrochemical cell, which contained the nickel hydroxide working electrode, a metal hydride electrode, a Hg/HgO reference electrode, and 6 M KOH solution as the electrolyte. As a comparison, pure nickel hydroxide tubes reported previously [15] and commercial spherical-powder (Tanaka Chemical, Japan) were also prepared into electrodes for electrochemical measurement. The discharge capacity of the nickel hydroxide in each positive electrode was calculated considering the amount of the active material $Ni(OH)_2$ only.

3. Results and discussion

3.1. Characterization of the as-synthesized product

The powder XRD pattern of the as-prepared $Y(OH)_3$-coated $Ni(OH)_2$ tubes is shown in Fig. 1. Nearly all the reflection peaks can be indexed as $Ni(OH)_2{\cdot}0.75H_2O$ (compared with the data of JCPDS file No. 38-0715) and $Y(OH)_3$ (ICDD-JCPDS card no. 09-0062). The remaining unmarked peaks may attribute to residual reactants or the remaining

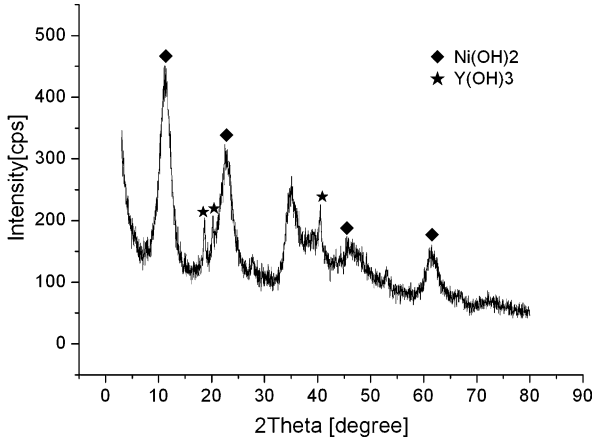

Fig. 1. XRD pattern of the $Y(OH)_3$-coated $Ni(OH)_2$ tubes.

alumina. Meanwhile, the broadening of peaks in the XRD spectra indicates that the crystalline size is very small.

Fig. 2 shows the EDS pattern of the obtained composite tubes. The presence of C and Cu in the EDS pattern is due to the copper mesh and carbon film, which were used as the TEM grid to support the sample. Al presence is owing to the trace remaining alumina. Based on the EDS analysis, the calculated weight ratio of $Ni(OH)_2$ and $Y(OH)_3$ is about 95:5.

Fig. 3 shows the SEM images of the sample at different magnifications. Fig. 3a is a front view of the product, from which it can be seen that a large quantity of tubular bundles were obtained. A remaining trace of the alumina matrix can be found inside the tube array, which is in agreement with the EDS analysis. This might be the reason why the tubes arranged parallel to one another. Fig. 3b shows that the $Y(OH)_3$-coated $Ni(OH)_2$ tubes are open-ended cylinders with smooth surface. The tubes are almost 200 nm in diameter, and this corresponds to the length of the pore size in the alumina template.

TEM and HRTEM images of the $Y(OH)_3$-coated $Ni(OH)_2$ tubes are shown in Fig. 4 to further investigate the detailed structure of the tubes. Fig. 4a shows TEM image of a group of

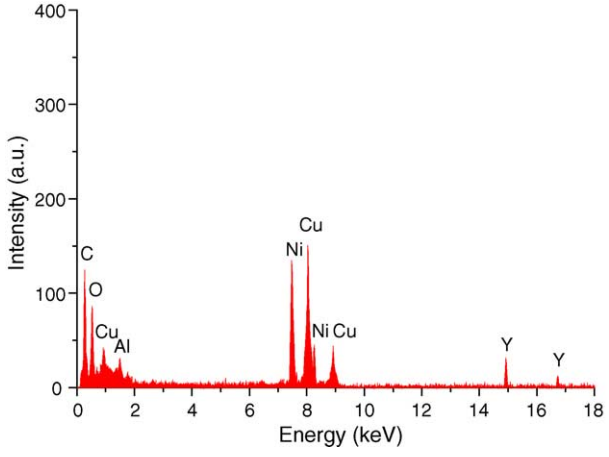

Fig. 2. EDS pattern of the obtained $Y(OH)_3$-coated $Ni(OH)_2$ composite tubes.

$Y(OH)_3$-coated $Ni(OH)_2$ tubes scattered on the copper mesh. The brightness difference between the center and the edge of the mesostructure confirms that the as-prepared samples are of hollow-tube morphology. It can be seen in Fig. 4b that the hollow tube has an outer diameter of about 200 nm and a wall thickness of 30–40 nm. This agrees with the SEM measurement. HRTEM image (Fig. 4c) shows the layer structure of the composite tubes, which presumably compose of an outer thin layer of $Y(OH)_3$ and an inner relatively thick layer of $Ni(OH)_2$. On the basis of the SEM and TEM observations, the proportion of the tube morphology was estimated to be about 95%. As a result, the size of the tubes is definitely of mesoscale dimension under our synthesis conditions.

3.2. Electrochemical measurement

Fig. 5 shows the first cyclic voltammograms of the three electrodes made by the $Y(OH)_3$-coated $Ni(OH)_2$ tube (A), pure $Ni(OH)_2$ tube (B), and spherical $Ni(OH)_2$ powder (C). Similarly shaped voltammograms were also obtained from the second to the fifth cycle, which is not shown here. Reversible peaks can be observed for these three electrodes, but their characteristics differ greatly from each other. The data in Fig. 5 are listed in Table 1 in more detail. As seen in Fig. 5, two peaks appeared when the electrodes were scanned cathodically, which can be assigned to the oxidation potential E_O and oxygen-evolution potential E_{OE}, respectively. During the following anodic process, only one peak was observed, which was generally named reduction potential E_R. The difference between E_O and E_R, namely $E_O - E_R$, is always taken as an estimate of the reversibility of the electrode reaction [16,17]. Smaller $E_O - E_R$ value indicates more reversible electrode reaction. Note that, the $E_O - E_R$ value of B is almost two times that of A, and C is nearly three times larger compared with A. It is also obvious that the relative intensities of E_O and E_R for A are much higher than C, which indicates that the energy transfer occurred in the reaction is higher. Meanwhile, the value of $E_{OE} - E_O$ for A increased greatly in comparison with that of B and C. This value is also an important parameter for judging the performance of the nickel electrode. The large value allows the electrode to be charged fully before oxygen evolution. Consequently, it can be deduced that the $Y(OH)_3$-coated $Ni(OH)_2$ tube electrode exhibits much better electrochemical cycling properties than that of the spherical-powder and pure $Ni(OH)_2$ tube electrodes.

Table 1
Experimental data summary from the cyclic voltammetric measurements

Electrode	Potentials (mV)				
	E_R	E_O	E_{OE}	$E_O - E_R$	$E_{OE} - E_O$
A	401	470	562	69	92
B	365	497	562	132	65
C	335	515	559	180	44

E_R: reduction potential; E_O: oxidation potential; E_{OE}: oxygen-evolution potential.

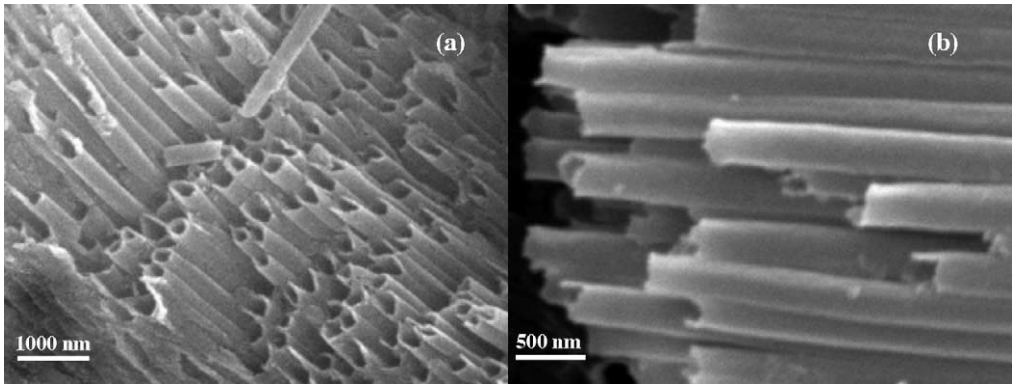

Fig. 3. Typical SEM images of the as-synthesized $Y(OH)_3$-coated $Ni(OH)_2$ tubes. (a) Overall view at low magnification; (b) side observation of the tube bundles.

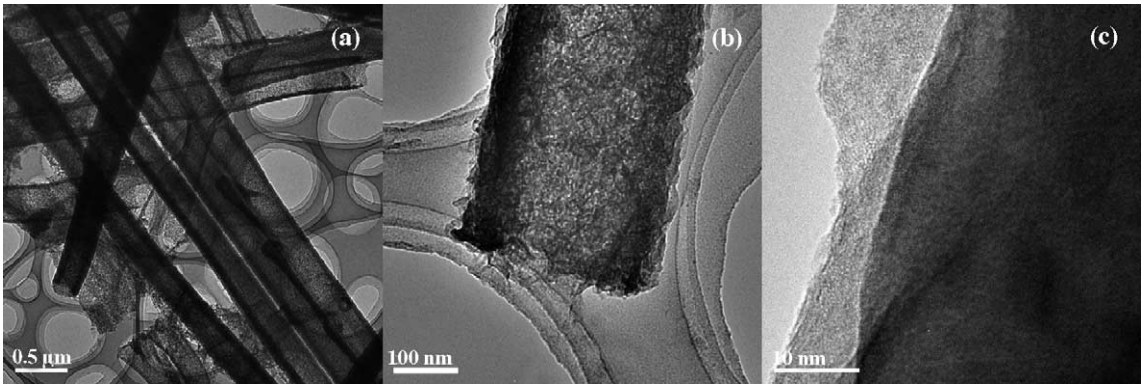

Fig. 4. Representative TEM (a, b) and HRTEM (c) images of the $Y(OH)_3$-coated $Ni(OH)_2$ composite tubes.

Fig. 6 shows the discharge curves of the $Y(OH)_3$-coated $Ni(OH)_2$ tube (A), pure $Ni(OH)_2$ tube (B) and spherical $Ni(OH)_2$ powder (C) electrodes in the tenth cycle. As seen from Fig. 6, the discharge capacity of A is 282 mAh g^{-1}, which is much higher than that of C (265 mAh g^{-1}). Furthermore, the discharge curve of A displays a higher discharge voltage than that of B and C. Thus, it can be concluded that much more active material can be utilized during discharge process in the electrode made by the $Y(OH)_3$-coated $Ni(OH)_2$ composite tube. Note that the highest discharge capacity of 315 mAh g^{-1} was obtained for the electrode made by the pure

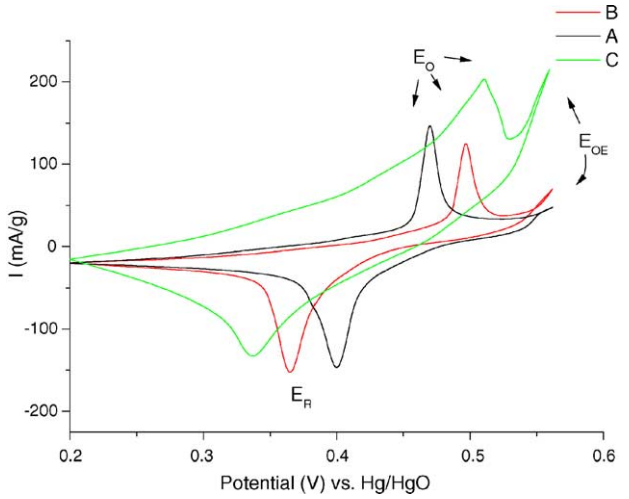

Fig. 5. Cyclic voltammograms of (A) $Y(OH)_3$-coated $Ni(OH)_2$ tube, (B) pure $Ni(OH)_2$ tube and (C) spherical-powder electrodes at 20 °C; scan rate: 0.5 mV s^{-1}.

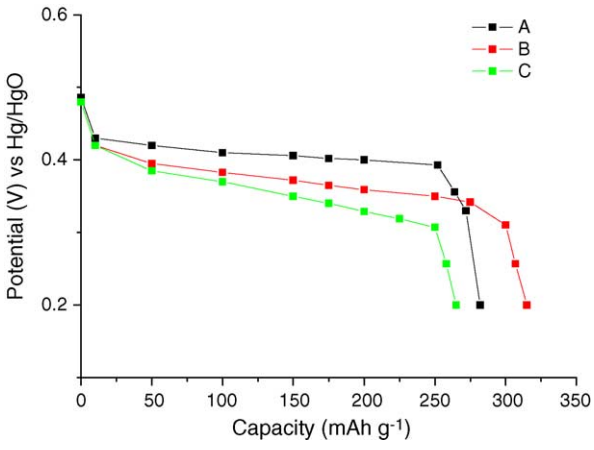

Fig. 6. Discharge curves for (A) $Y(OH)_3$-coated $Ni(OH)_2$ tube, (B) pure $Ni(OH)_2$ tube and (C) spherical $Ni(OH)_2$ powder electrodes at the discharge current density of 50 mA g^{-1} and 20 °C.

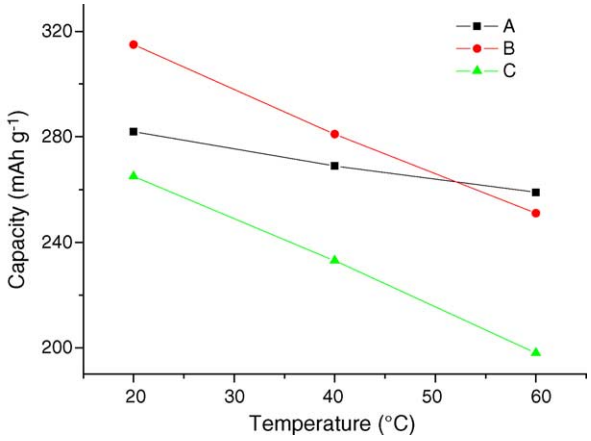

Fig. 7. Discharge capacities of the (A) $Y(OH)_3$-coated $Ni(OH)_2$ tube, (B) pure $Ni(OH)_2$ tube and (C) spherical $Ni(OH)_2$ powder electrodes at different temperatures with a discharge rate of 0.2 C.

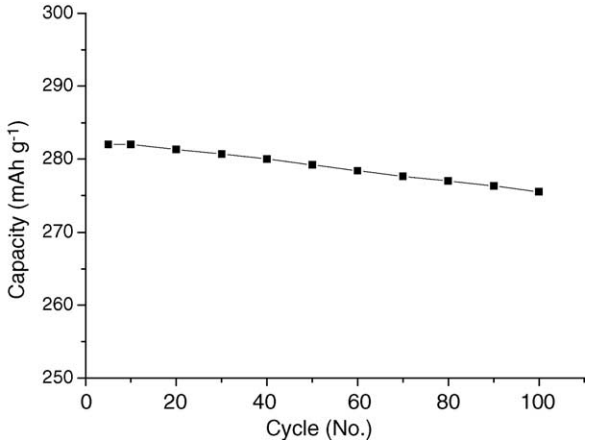

Fig. 9. Cycle life of the $Y(OH)_3$-coated $Ni(OH)_2$ tube electrode at 20 °C.

$Ni(OH)_2$ tubes. This indicates that in addition to the phase transformation of β-$Ni(OH)_2$ to β-NiOOH, partial formation of γ-NiOOH occurred.

Fig. 7 illustrated the effect of the working temperature on the electrode capacity at a discharge current density of 50 mA g^{-1}. At 60 °C, the $Y(OH)_3$-coated $Ni(OH)_2$ tube electrode still retained about 91.8% of the capacity at the discharge of 20 °C, while the pure $Ni(OH)_2$ tube electrode and spherical-powder electrode only showed 80.0 and 74.7% of their values at 20 °C, respectively. It can be seen that as the working temperature increases, the discharge capacity of the composite tube electrode decreases much more slowly than that of pure tube electrode and spherical-powder electrode.

The effect of the discharge current density on the electrode capacity at 20 °C is further illustrated in Fig. 8. It can be seen that the capacity of the composite tube electrode decreased more slowly with the increasing discharge current density compared with the pure tube electrode and the spherical-powder electrode. Therefore, the composite tube electrode exhibits much better electrochemical performance at high discharge current densities and at high working temperatures.

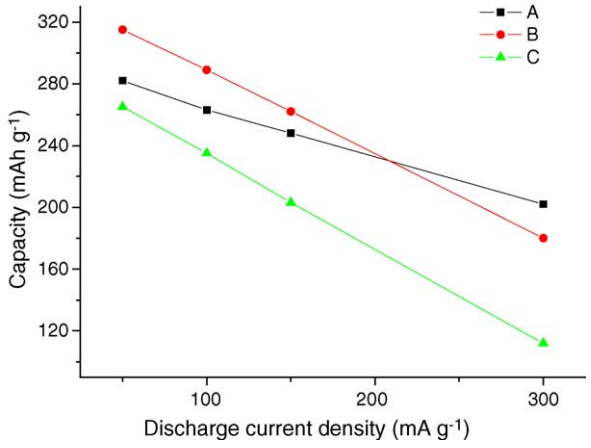

Fig. 8. Discharge capacities of the (A) $Y(OH)_3$-coated $Ni(OH)_2$ tube, (B) pure $Ni(OH)_2$ tube and (C) spherical $Ni(OH)_2$ powder electrodes at different discharge current densities with the temperature of 20 °C.

Since the $Y(OH)_3$-coated $Ni(OH)_2$ tube electrode shows excellent CV, high-rate discharge, and high-temperature working properties, its cycle life was further tested (Fig. 9). It can found that the capacity of the composite tube electrode decreased by only about 2.3% after a preliminary test of 100 charge/discharge cycles at 50 mA g^{-1} with 100% depth of charge and discharge. An average capacity fading of 0.065 mAh g^{-1} per cycle occurred, indicating a high stability of the composite tube during the cycling process.

The interesting question is why the $Y(OH)_3$-coated $Ni(OH)_2$ tube electrode shows better comprehensive performance. An interpretation follows. The as-synthesized $Y(OH)_3$-coated $Ni(OH)_2$ tube has a small crystal size and large surface area, which helps to enhance the contact between the active material and the electrolyte. Meanwhile, the hollow structure of the tube allows diffusion to occur easily. As shown in Fig. 10, ionic diffusion can proceed along both sides of the tube walls, while it can merely occur through the surface of the sphere. As we know that the step of the proton diffusion is the rate-determining step in nickel hydroxide electrode [18], it is thus that the increase of the rate of the proton diffusion results in the decrease of electrode polarization. In addition, the coated $Y(OH)_3$ may suppress γ-NiOOH formation during charge–discharge cycling. This may decrease the electrode capacity but it can improve the utilization of the active material. Furthermore, the composite tube structure with $Y(OH)_3$ coating may cause changes in the electronic properties and act as a barrier for electron transfer in the oxygen-evolution process, which contributes to superior electrode performance at high current density and high-temperature. Accordingly, the excellent behavior of $Y(OH)_3$-coated $Ni(OH)_2$ tube electrode is reasonable and readily understood.

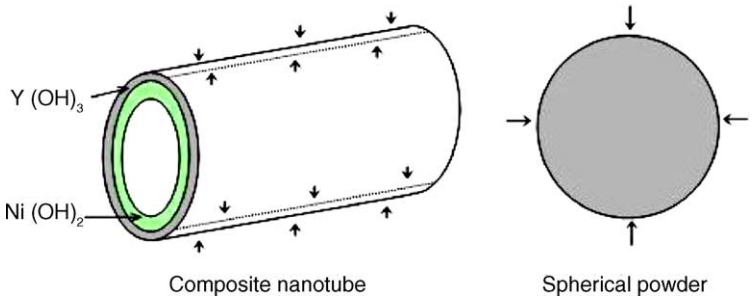

Fig. 10. Sketch diagram showing the diffusion comparison in a tube and a spherical-powder.

It is highly noted that polymer and block copolymer have been recently employed as soft templates [19] in preparing nanomaterials in order to meet the needs of practical application. Our further work is focused on utilizing certain soft templates to substitute alumina membranes for synthesizing $Y(OH)_3$-coated $Ni(OH)_2$ tubes and other composite tubes in large-scale production.

4. Conclusions

$Y(OH)_3$-coated $Ni(OH)_2$ tubes were prepared by a template method under ambient conditions. XRD, EDS, SEM, TEM, and HRTEM measurements showed that the composite tube structure composes of $Y(OH)_3$ and $Ni(OH)_2$ layers and the tube is of mesoscale dimension. Electrochemical measurements revealed that the composite tube electrode exhibits excellent charge/discharge performance, especially at high-rate and high-temperature working. Therefore, $Y(OH)_3$-coated $Ni(OH)_2$ tubes are promising as the positive-electrode materials of alkaline rechargeable batteries.

Acknowledgements

This work was supported by the NSFC (20325102 and 90406001) and TCTPF-Key Project (200248 and 104055).

References

[1] T. Sakai, M. Matsuoka, C. Iwakura, in: K.A. Gschneidner Jr., L. Eyring (Eds.), Handbook on the Physics and Chemistry of Rare Earths, vol. 21, Elsevier Science B.V., Amsterdam, 1995, p. 133.
[2] M.S. Dresselhaus, I.L. Thomas, Nature 414 (2001) 332.
[3] D. Linden, Handbook of Batteries, McGraw-Hill, New York, 2002.
[4] H. Bode, K. Dehmelt, J. Witte, ELectrochim. Acta 11 (1966) 1079.
[5] R. Barnard, C.F. Randell, F.L. Tye, J. Appl. Electrochem. 10 (1980) 109.
[6] D. Singh, J. Electrochem. Soc. 145 (1998) 116.
[7] C. Faure, C. Delmas, P. Willmamn, J. Power Sources 36 (1991) 497.
[8] M. Oshitani, M. Watada, T. Tanaka, T. Iida, in: P.D. Bennett, T. Sakai (Eds.), Hydrogen and Metal Hydride Batteries, vols. 94–27, The Electrochem. Soc. Inc., Pennington, NJ, 1994, p. 303.
[9] E. David, J. Alvin, R. Peter, T. Xiao, J. Power Sources 65 (1997) 231.
[10] J. Chen, D.H. Bradhurst, S.X. Dou, H.K. Liu, J. Electrochem. Soc. 146 (1999) 3606.
[11] M. Oshitani, M. Watada, K. Shodai, J. Electrochem. Soc. 148 (2001) A67.
[12] X. Mi, X.P. Gao, C.Y. Jiang, M.M. Geng, Electrochimica. Acta 49 (2004) 3361.
[13] K. Watannabe, T. Kikuoka, J. Appl. Electrochem. 25 (1995) 219.
[14] X. Wang, H. Luo, P.V. Parkhutik, A.C. Milan, E. Matveeva, J. Power Sources 115 (2003) 153.
[15] F.S. Cai, G.Y. Zhang, J. Chen, Angew. Chem. Int. Ed. 43 (2004) 4212.
[16] P.V. Kamath, M.F. Ahmed, J. Appl. Electrochem. 23 (1993) 225.
[17] D.A. Corrigan, R.M. Bendert, J. Electrochem. Soc. 136 (1989) 273.
[18] S. Motupally, C.C. Streiz, W.J. Weidner, J. Electrochem. Soc. 145 (1998) 29.
[19] K.J.C. Bommel, A. Friggeri, S. Shinkai, Angew. Chem. Int. Ed. 42 (2003) 980.